International Journal of Heat and Mass Transfer 52 (2009) 3427–3438

Contents lists available at ScienceDirect

International Journal of Heat and Mass Transfer

journal homepage: www.elsevier.com/locate/ijhmt

Numerical model of gaseous fuel jet injection into a fluidized furnace

Stevan Nemoda, Milica Mladenović, Srdjan Belošević, Rastko Mladenović *, Dragoljub Dakić

Institute of Nuclear Sciences "Vinča", Laboratory of Thermal Engineering and Energy, P.O. Box 522, 11001 Belgrade, Serbia

ARTICLE INFO

Article history:
Received 11 July 2008
Accepted 12 February 2009
Available online 3 May 2009

Keywords:
Model
Fluid fuel
Jet injection
Fluidized bed

ABSTRACT

The paper presents a fluid-porous medium model, developed for stationary 2D predictions of fluidized bed. Dense phase is considered a fixed porous medium, while gas–particle interactions and bubbling phase are modeled regarding balance of friction forces between gas and particles. Like referent measurements, predictions of lateral jet injection into the bed suggest the jet penetration length is strongly affected by fluid velocity at the nozzle outlet, while influences of the nozzle vertical position and inclination angle are not significant. Also, the fluid velocity and the nozzle vertical position exert pronounced effects on mixing rate of components (fuel and oxidizer).

1. Introduction

Bubbling fluidized bed (FB) is of great importance in process engineering and energy. In the last 40 years, due to the increasing energy crisis and need for environmental protection, its application has been growing rapidly. Well-known hydrodynamics and thermal properties of FB, i.e. good conductivity, intensive heat transfer as well as great thermal capacity, offer the possibility of numerous chemical reactions that can take place between various materials.

For the purpose of investigation in energy and process engineering, besides the experimental methods, numerical simulation is used. Its advantages are savings in means and time during the process of development of facilities and technologies in this field. However, numerical tool for simulation of processes which include FB is not completely developed, due to the difficulties in describing a relatively complex flow and peculiarities in heat and mass transfers that exist in gas–particles fluidized systems. Besides that, the majorities of existing numerical tools are complex and require expensive computer hardware, so they are not appropriate for the needs of investigation and engineering. Numerical models aimed for simulation of processes in FB, developed so far, belong either to the Lagrangian models [1,2], where each particle, representing a characteristic group of particles, is tracked numerically during its motion within FB, or to the Eulerian models, where regions of the flow domain, through which gas or particles flow, are considered. Lagrangian approach to the simulation of particle motion in FB is more exact, but in most cases not suitable for development- investigations, for it requires considerable computation time and memory capacity. Eulerian approach to the FB modeling is used by more authors and it provides relatively simpler numerical solutions. The so-called two-fluid modeling approach is of special importance [3,4], where gas and dense phase of FB (gas–particles system at conditions of minimal fluidization) are considered as two fluids with different characteristics. In momentum conservation equations for an effective fluid (presenting a dense phase of FB), fluid–particle interaction at conditions of minimal fluidization is modeled, as well as interaction between particles.

This work suggests to some extent a numerically simpler version of two-fluid models, where dense phase of FB is considered as a fixed porous medium. Gas–particle interactions, as well as conditions for occurrence of bubbles and non-particle zones are modeled in similar way as by the two-fluid models, except from excluding the simulation of particle motion, i.e. dense phase.

This kind of approach to the FB modeling enables computationally efficient engineering calculations of fluidizing medium conditions, with analysis of locations and average sizes of non-particle zones that can provide a number of information useful during planning of processes in FB. An example of the application of suggested method for FB modeling, which is the subject of this work, is a numerical simulation of fluid lateral jet injection into the FB, for the purpose of rapid and simple determination of the jet penetration length into the FB and the efficiency of mixing between injected fluid component and dense phase. This analysis is very useful in trying to find the solutions for combustion of liquid and gaseous fuel in the FB reactor. Given numerical method enables a rapid and relatively simple analysis of possible technical solutions for injection of fuels with different heat capacities into the FB reactor, e.g. fuel injection by using different inclination angles and positions of the nozzle, providing

* Corresponding author. Tel.: +381 11 3408217/8066611; fax: +381 11 2453670.
E-mail address: rastkom@vin.bg.ac.yu (R. Mladenović).

0017-9310/$ - see front matter © 2009 Elsevier Ltd. All rights reserved.
doi:10.1016/j.ijheatmasstransfer.2009.02.045

Nomenclature

Latin symbols

d_j	nozzle opening diameter (m)
d_p	particle mean diameter (m)
f	components mixing fraction (–)
g	gravity (m s^{-2})
h	nozzle-bed bottom distance (m)
h_0	fluidized bed height (m)
$K_{1,i}$	laminar flow permeability in the direction i (m^2)
$K_{2,i}$	turbulent flow permeability in the direction i (m)
k	turbulent kinetic energy (m^2 s^{-2})
L_j	jet penetration length (m)
p	pressure (Pa)
U_j, U_i	components of fluid average velocity vector (m s^{-1})
U_j	velocity at the nozzle outlet (m s^{-1})
U_{mf}	minimum fluidization velocity (m s^{-1})
U_s	gas velocity at a free cross-section above the bed (m s^{-1})
x_i, x_j	coordinates (m)
z	components mixing factor $(1 - \lvert f^{st} - f\rvert / f^{st})$ (–)

Greek symbols

α	nozzle inclination angle (rad.)
ε	turbulent kinetic energy dissipation (m^2 s^{-3})
ε	porosity (–)
μ	dynamic viscosity (kg m^{-1} s^{-1})
μ_t	dynamic turbulent viscosity (kg m^{-1} s^{-1})
μ_{eff}	effective dynamic viscosity (kg m^{-1} s^{-1})
ρ	fluid density (kg m^{-3})
ρ_b	fluidized bed deposited density (kg m^{-3})
ρ_f	fluidization gas density (kg m^{-3})
ρ_j	gas density in the nozzle (kg m^{-3})
ρ_s	particle material density (kg m^{-3})
ψ_{fr}	effective friction coefficient (–)

simultaneously as efficient mixing with FB inert material as possible.

For the purpose of making the aforementioned analyses, a 2D numerical model has been developed for simulation of gas jet entrainment into the bed of particles fluidized by means of air. A series of numerical experiments has been performed to analyze the dependence of lateral jet penetration length into the FB on different parameters of jet injection, such as: the jet injection velocity, the nozzle inclination angle and the height of the nozzle position within the FB. In order to verify the suggested model, the results of numerical simulation are compared with experimental ones [5]. The lateral jet penetration length is an important condition for good mixing of components and, accordingly, also for the efficient and stable combustion of lateral jet of fuel, especially when we are dealing with liquid and pulverized solid fuel, where homogeneous dispersion of drops (particles) within the whole volume of the furnace is very important. When gaseous fuel is in question, i.e. evaporated components of liquid fuel, besides the jet penetration length it is important to analyze flow characteristics, diffusion and mixing intensity of gaseous fuel components and oxidizers. Because of that, the suggested model of jet penetration into the FB is complemented with a set of transport equations for convection and diffusion of gaseous components in the non-particle flow-porous medium system. Accordingly, a series of numerical experiments have been performed for a multi-component system with jet entrainment into the FB. The obtained results have confirmed the assumption that taking into account the components mixing efficiency as a relevant factor, in addition to the jet penetration length, is essential in predicting the fluidized furnace performance.

The model of fluidization has been simplified to a considerable extent because it is aimed only for the simulation of the jet penetration into the fluidized bed (FB). So, in this case, it is not necessary to consider the momentum, heat and mass transfer of the particle (dense) phase. The interaction between the gas flow and the particle phase has been considered in details by the suggested model, taking into account also the motion (oscillations) of the particles, through the semi-empirical expression for the effective friction coefficient, as a function of the fluidization number, as explained later. For the same reason – lack of interest for detailed consideration of the flow processes within the particle (dense) phase, the standard k–ε turbulence model has been used, providing a detailed description of flow within the jet flow zone.

2. The fluidization model and the fluid-porous medium method

As the majority of two-fluid models, the suggested numerical model of FB is based on the assumptions of Davidson's [6] two-phase fluidization model. According to the suggested model, the gas flow through the particle (dense) phase and the bubble zone (non-particle zone) is observed. The volume zones with and without particles are defined on the basis of the gas–particle phase interaction model. The non-particle zones (bubbles) are considered as the turbulent gas flow, while the dense phase is modeled with respect to the models of flow in porous media.

The flow in FB is described by means of the momentum conservation equations for turbulent flow, in conjunction with the continuity equation, with the correction of pressure drop for particles-containing zones at the conditions of minimum fluidization velocity (dense phase of the FB). In common models of flow in porous media, the flow is assumed to be laminar, because of a very narrow space between particles, i.e. narrow passage for fluid flow. However, in addition to the non-particle zones (bubbles), the flow is assumed to be turbulent also in the zones of dense phase, because the particles at the conditions of minimum fluidization velocity are in the state of chaotic motion and that is the reason to assume turbulent flow between them. Prediction of the positions and sizes of bubble-zones (i.e. non-particle zones) is performed by setting the balance of friction forces between the particles and the fluid, taking into account the forces of particles interactions.

All the calculations are stationary, so the model offers the possibility to obtain an average image of flow in the FB with locations and shapes of the most frequently observed non-particle zones.

2.1. Equations of the model

All parts of the model have been developed for the case of a two-dimensional plane flow. All differential equations of the model are elliptical.

Turbulent fluid flow can be described satisfactorily with time-averaged Navier–Stokes equations and the k–ε turbulence model for determination of turbulent stresses [7]. In the proposed calculation, the equations for time-averaged variables (U, V, p) are solved, and Reynolds stresses are modeled based on the hypothesis of isotropic turbulent viscosity:

$$-\overline{\rho uv} = \mu_t\left(\frac{\partial U_j}{\partial x_i} + \frac{U_i}{\partial x_j}\right) \tag{1}$$

Turbulent viscosity is determined from the k–ε turbulence model:

$$\mu_t = C_\mu \frac{\rho k^2}{\epsilon}, \quad \mu_{eff} = \mu + \mu_t. \tag{2}$$

In this way, the calculation includes solving two additional equations: for k and ε.

The main conservation equations, given in tensor notation, are:

Continuity equation

$$\frac{\partial}{\partial x_j}(\rho U_j) = 0. \tag{3}$$

Momentum transfer for the gas phase in i-direction

$$\frac{\partial}{\partial x_j}(\rho U_j U_i) - \frac{\partial}{\partial x_j}\left(\mu_{eff}\frac{\partial U_i}{\partial x_j}\right) = -\frac{\partial p}{\partial x_i} + \frac{\partial}{\partial x_j}\left(\mu_{eff}\frac{\partial U_j}{\partial x_i}\right) - \frac{2}{3}\frac{\partial}{\partial x_i}\left(\mu_{eff}\frac{\partial U_k}{\partial x_k}\right). \tag{4}$$

Momentum transfer for the dense phase in i-direction

$$\frac{\partial}{\partial x_j}(\rho U_j U_i) - \frac{\partial}{\partial x_j}\left(\mu_{eff}\frac{\partial U_i}{\partial x_j}\right) = -\frac{\partial p}{\partial x_i} - \left(\frac{\mu}{K_{1,j}}U_j + \frac{\rho}{K_{2,j}}U_j|U_j|\right) + \frac{\partial}{\partial x_j}\left(\mu_{eff}\frac{\partial U_j}{\partial x_i}\right) - \frac{2}{3}\frac{\partial}{\partial x_i}\left(\mu_{eff}\frac{\partial U_k}{\partial x_k}\right). \tag{5}$$

Turbulent energy

$$\frac{\partial}{\partial x_j}(\rho U_j k) - \frac{\partial}{\partial x_j}\left(\frac{\mu_{eff}}{\sigma_k}\frac{\partial U_i}{\partial x_j}\right) = G_{k_1} - \rho\varepsilon. \tag{6}$$

Dissipation of turbulent energy

$$\frac{\partial}{\partial x_j}(\rho U_j \varepsilon) - \frac{\partial}{\partial x_j}\left(\frac{\mu_{eff}}{\sigma_\varepsilon}\frac{\partial U_i}{\partial x_j}\right) = \frac{\varepsilon}{k}(C_1 C_{k_1} - C_2\rho\varepsilon). \tag{7}$$

where the production of turbulence kinetic energy is given as:

$$G_{k_1} = \mu_{eff}\left\{2\left[\left(\frac{\partial U_j}{\partial x_j}\right)^2 + \left(\frac{\partial U_i}{\partial x_j}\right)^2\right] + \left(\frac{\partial U_j}{\partial x_i} + \frac{\partial U_i}{\partial x_j}\right)^2\right\}.$$

Constants of the turbulence model, which correspond to standard values from literature [8], are given in Table 1.

Flow in the dense phase zones of the FB is modeled in accordance with the models of porous media. It is assumed that the dense phase is pseudo-homogeneous with a constant averaged density, where the gas–particles system is looked upon as one single phase. Accordingly, the flow inside the zones surrounded by porous matrices can be modeled by similar equations as in the case of single-phase flow, with necessary corrections (Eq. (5)). The essential correction of these equations refers to the additional term which defines the pressure drop through the porous medium, i.e. the FB dense phase. The additional term in the momentum transport equation, in the zones with the dense phase, is modeled in accordance with the Forchheimer's equation:

$$\frac{\partial p}{\partial x_i} = -\frac{\mu}{K_{1,i}}U_j - \frac{\rho}{K_{2,i}}|U_j|U_j, \tag{8}$$

Table 1
Constants of the k–ε turbulence model.

C_μ	C_1	C_2	σ_k	σ_ε	σ_h	C_μ
0.99	1.44	1.92	1	1.3	0.9	0.09

where U_j stands for the gas velocity per reactor cross-section. Tensors $K_{1,i}$ and $K_{2,i}$ are linear and turbulent permeability coefficients, respectively. These coefficients, for FB dense phase conditions, are defined according to the Ergun equation as follows:

$$K_{1,i} = \frac{\varepsilon^3 d_p^2}{150\cdot(1-\varepsilon)^2}, \tag{9}$$

$$K_{2,i} = \frac{\varepsilon^3 d_p}{1.75\cdot(1-\varepsilon)}. \tag{10}$$

2.2. Numerical procedure and boundary conditions for homogeneous flow domain

Differential conservation equations (3)–(7) are non-linear and mutually coupled. Numerical procedure of solving the equations has been performed by using the control volume method [8], including the collocated numerical grid for momentum equations, hybrid numerical scheme (the combination of upstream and central differencing) and SIMPLE algorithm for solving the equations [8]. The iteration process stabilization is done by sub-relaxation technique. The calculation procedure and the numerical method are described in more details in [7].

For elliptical type of equations (3)–(7), it is necessary to define the conditions at all boundaries of the space considered, i.e. inlets, outlets and solid walls. At the inlets, the desired boundary flow conditions are set. At the outlet cross-section, the axial gradients of all variables are set to zero. At the walls, a logarithmic velocity profile is presumed, with corresponding friction stress dependences.

2.3. Modeling of the bubble phase zones

According to the model proposed, zones without particles are represented in locations where the intensity of the gas–particle interaction forces is higher than the intensity of interaction forces among the particles themselves. With some simplifications, the gas–particles interaction forces can be reduced to the force of friction between gas and particles in the FB dense phase and determined according to the Ergun equation, by means of the expressions (8)–(10).

Interactions between particles can be reduced to the inter-particle friction force and to the effects of inter-particle collisions in the FB. These two effects can be modeled together, with the expression for the effective inter-particle friction force:

$$F_p = \frac{\partial p_f}{\partial x_i} = \psi_{fr}\rho_s(1-\varepsilon_b)g, \tag{11}$$

where term $\rho_s(1-\varepsilon_b)g$ refers to the pressure of the deposited bed of particles over the bed differential height, and ψ_{fr} is the effective friction coefficient of the bed particles, which at the same time refers to the effects of collision between the fluidized bed particles and is defined by the following semi-empirical expression:

$$\psi_{fr} = a\cdot(U_s/U_{mf})^b, \tag{12}$$

where a and b are empirical constants.

As it can be observed from the expression (12), the coefficient ψ_{fr} depends on particle characteristics (material, shape, specific area etc.), included in the constant a, as well as on the fluidization number (U_s/U_{mf}), which is the measure of FB agitation, i.e. the intensity of inter-particle collisions.

If the condition $\partial p/\partial x_i > F_p$ is met inside a section of the observed space (control volume), then, according to the proposed model, it is adopted that the given zone belongs to the bubble phase, while sections of the calculation space with $\partial p/\partial x_i \leqslant F_p$ correspond to

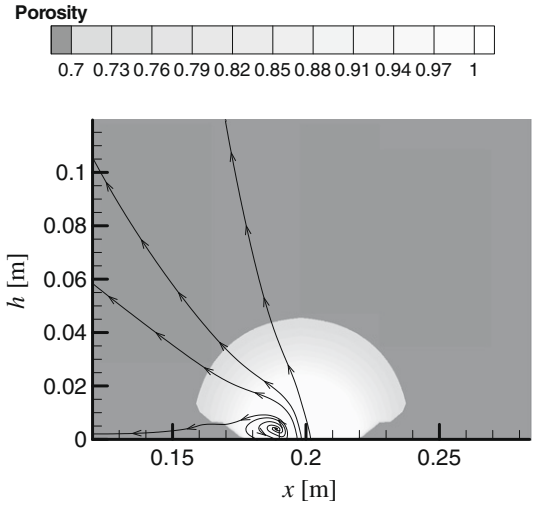

Fig. 1. Numerical simulation of the bubble phase appearance in the FB.

the FB dense phase. The porosity inside the bubble phase can be determined by applying the Todes's semi-empirical expression [9]:

$$\varepsilon_b = \varepsilon_{mf}\left(\frac{Re + 0.02Re^2}{Re_{mf} + 0.02Re_{mf}^2}\right)^n, \tag{13}$$

where Re_{mf} and ε_{mf} refer to Reynolds number and porosity, respectively, under the conditions of minimum fluidization velocity, and n stands for an empirical constant equal to 0.21, according to [9].

In general case, porosity of the bubble phase, determined by the suggested model (10)–(13), could be in the range from ε_{mf} to 1 (Fig. 1); at first, the boundaries of the bubble phase are determined by means of the procedure (10)–(12), while the distribution of the porosity within this zone is calculated by semi-empirical expression (13). Numerical prediction of the jet penetration length into the FB is performed by means of the same model (10)–(13), but for the jet boundaries only the bubble zone region has been taken into account, in which, according to the model, the porosity is equal to 1.

An illustration of the shown numerical simulation procedure is given in Fig. 1, which depicts the appearance of the bubble phase inside the dense phase of the FB, in the case of the air jet entry through the opening with 0.004 m in diameter, with the velocity of 5 m/s, into the fixed bed of sand particles, with a mean diameter of 300 μm.

2.4. Numerical procedure of the bubble phase zones determination

Within an iterative procedure of solving the system of the conservation equations (3)–(7), it is almost impossible to confine the zone without the particles at the same time, i.e. it is impossible to track the bubble growth and to form the flow through the zones of the bubbles and particles simultaneously, with the full convergence accomplished. For this reason, the following procedure has been used: at first, an iterative procedure is performed to solve the system of the conservation equations (3)–(7), assuming that the entire calculation domain is filled with the particle phase (like porous matrix with given porosity), with the gas jet inflow. When the full convergence is achieved, a special subroutine is used to analyze the calculation domain parameters, in accordance with the bubble zone determination model (10)–(12) and the values of porosity in the corresponding control volumes are determined with respect to the model (13). After these calculations, the iterative procedure of solving the system of the conservation equations (3)–(8) is performed again, but for the calculation domain in which the bubble zones are defined in addition to the porous medium. During the iterations, the boundary conditions (10)–(13) are included again, for the sake of control and eventual corrections of the zones formed.

The gas flow boundary conditions are identical for non-particle zones as for the particle phase zones, with application of an additional term (8) for correction of the pressure drop in Eq. (5), which is defined, in this case, by the expressions (8)–(10). At the inlets, the desired boundary flow conditions are set. At the outlet cross-section, the axial gradients of all variables are set to zero. At the walls, a logarithmic velocity profile is presumed, with corresponding friction stress dependences.

3. The formulation of the problem

The proposed model for numerical simulation of fluid-dynamic phenomena in the fluidized bed is very suitable for application when solving the problem of optimizing the procedure of lateral stream introduction into the FB. The key issue with fluidization furnaces with jet fuel feeding is to achieve as uniform mixing of the combustible dispersion with FB inert material as possible. Uniform fuel mixing in FB depends on the penetration of the lateral jet into the reactor, which can be controlled by a number of parameters, the most important being the following ones: gas velocity at the nozzle outlet, the nozzle position and the inclination angle of the jet towards the direction of the fluidization gas. By applying the proposed computation tool, numerical experiments can be carried out, in order to examine the influence of these parameters on the jet penetration into the FB, which makes possible to neglect or minimize the expensive experimental procedures and operations.

Results of extensive experimental investigations of the penetration of lateral air jet into the fluidized bed have been given in [5]. Experiments were conducted on a Plexiglas set-up with a two-dimensional FB, 314 mm wide and 25 mm thick, with the possibility to change the position and the inclination of the lateral jet. The lateral jet penetration length into the FB was measured by a camcorder, with the photo-shooting frequency of 25 pictures per second. The measurement error for the jet penetration length, obtained by this procedure, was not higher than 5 mm.

The experimental results have been compared to the calculations done with the numerical model shown in this contribution. It is obvious that, for the simulation of given experiments, two-dimensional calculations can be applied.

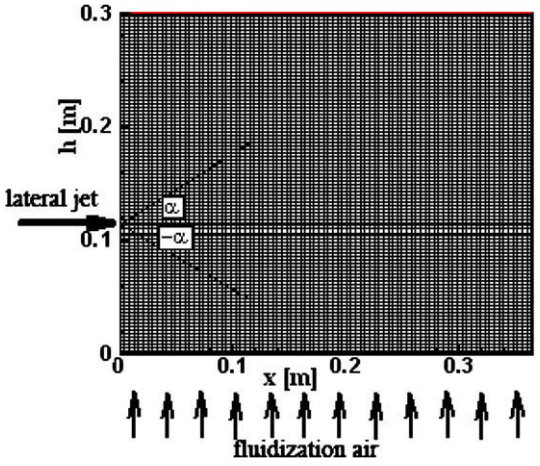

Fig. 2. Numerical grid scheme and boundary conditions.

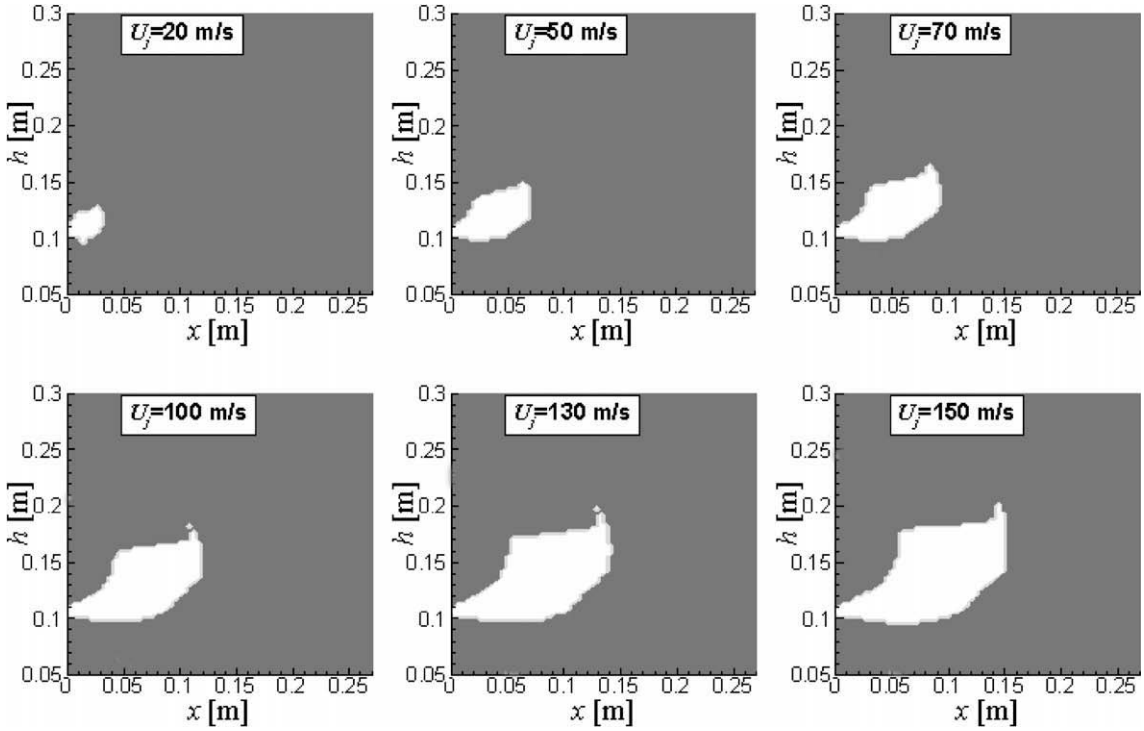

Fig. 3. Numerical simulation of the jet penetration into the FB.

For the purposes of the calculations, a numerical grid, shown in Fig. 2, containing 9604 nodes, has been used. The whole calculation zone consists of the fluidized bed with the existence of bubble and dense phases, with their distribution being determined by the proposed model. A uniform fluidization air distribution has been presumed, having in mind that the place of fluidization air introduction has the properties of the solid wall.

4. Calculation results for the jet penetration and comparisons with the experiments

In Fig. 3, the results of a numerical simulation of a series of experiments from [5], obtained by applying the described numerical tools, are given. The simulated experiments refer to the investigation of the influence of nozzle outlet velocity on the penetration effect of a horizontal jet in FB. The fluidization gas, as well as the fluid inside the nozzle, was air at room temperature. The inert FB material consisted of millet grains with medium diameter of 1.43 mm and density of 1402 kg/m^3. The dimensions of the working space were in accordance with the scheme in Fig. 2. Air velocities at the horizontal nozzle outlet (9 mm in diameter) were in the range between 20 and 150 m/s. The fluidization number during all experiments was $U/U_{mf} = 3$, with the medium porosity of the bed, surrounding the jet, equal to 0.6.

The jet velocity at the nozzle outlet, as it can be observed from Fig. 3, has a strong influence on the jet penetration length, which is in accordance with the general conclusion of the experiments. Based on experimental results, a dependence correlation of the horizontal jet penetration length into the FB as a function of fluidization parameters and nozzle characteristics is proposed in [5]:

$$\frac{L_j}{d_j} = 1.89 \times 10^6 \cdot \left[\frac{\rho_j U_j^2}{(1-\varepsilon_b)\rho_s g d_p}\right]^{0.327} \cdot \left(\frac{\rho_f}{\rho_s}\right)^{1.974} \cdot \left(\frac{d_p}{d_j}\right)^{-0.04} - 3.8. \quad (14)$$

Comparison of the numerical model with experimental results was performed by analysis of the dependence of maximum dimensionless penetration distance (L_j/d_j) of the jet into the FB on the following: the nozzle outlet air velocity (U_j), the nozzle inclination angle (α) and the nozzle-bed bottom distance (h), under the constant parameters of fluidization. The comparison of the computer simulation of the horizontal jet penetration length as a function of air velocity inside the nozzle, with the experimental results from [5], is given in Fig. 4a. In this figure, numerically obtained dependences of the dimensionless jet penetration distance on the jet velocity entering the FB, have been compared with experimental results and values obtained by correlation (14). Numerical calculation results are in very good accordance with the experiments and the correlation (14), especially for the nozzle velocity values in the range of 40–120 m/s. It should be noted here that, for numerical calculation purposes, the values of constants applied, from (12), are: $a = 0.65$ and $b = 1.5$. The given values of the constants a and b have been selected on the basis of series of numerical experiments, compared with experimental measurements taken from [5]. It can be said that the chosen values of the constants show important universality, because they have been validated for quite a number of cases with different parameters of fluidization and penetrating jet, such as: materials and diameters of the FB particles, the nozzle diameters, inlet velocities and inclination angles of the jet, etc.

The suggested model of jet penetration into the FB has been validated also against a well tested semiempirical model of gaseous jet entrainment into the FB (proposed by Yates et al. and discussed in [10]), with the comparison given in Fig. 4b. It should be pointed out that these calculations have been performed with respect to the vertical position of the nozzle (upflowing jet), so that the numerical model has been adjusted accordingly, i.e. the flow is considered as shown in Fig. 1. The rest of the parameters, like the conditions for fluidization and the nozzle dimensions, are exactly the same as in the calculations and experiments, with the results given in Fig. 4a. As shown in Fig. 4b, quite acceptable

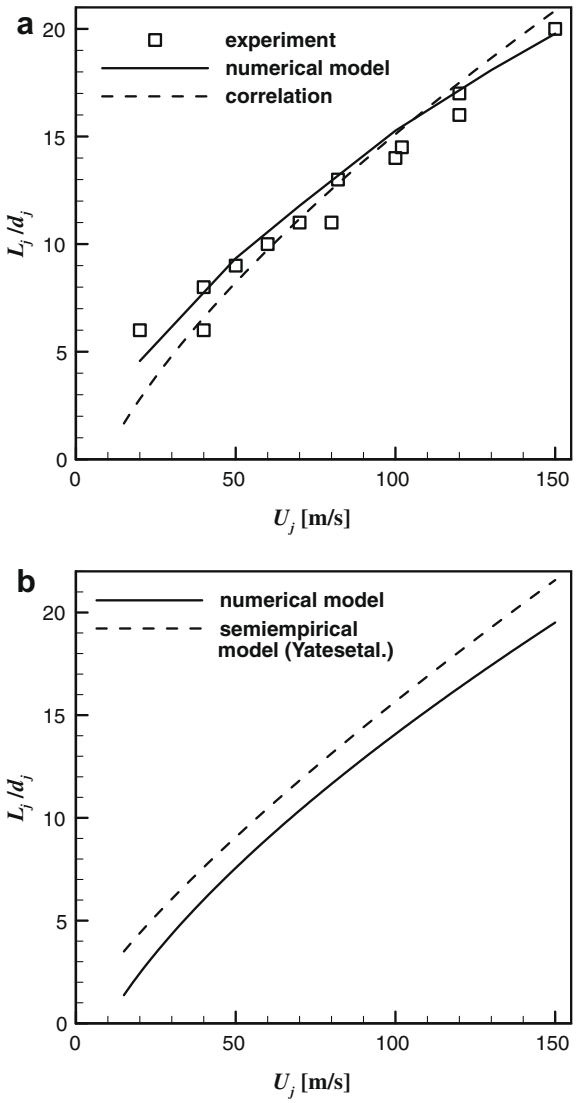

Fig. 4. Dimensionless jet penetration lengths as a function of air velocity inside the 9 mm nozzle, at fluidization number equal to 3.

agreement between the model suggested in the paper and the semiempirical model given in [10] has been obtained.

In addition to the lateral jet analysis, a series of experiments was done in [5], investigating the influences of the nozzle inclination angle (α in Fig. 2) and of the jet introduction height on the jet penetration into the FB. As a result of these investigations, a correlation based on experimental results was proposed, giving a dependence of the inclined jet penetration length into the FB as a function of fluidization parameters and the nozzle characteristics:

$$\frac{L_j}{d_j}+3.8=1.64\times10^6\cdot\left[\frac{\rho_j U_j^2}{(1-\varepsilon_b)\rho_s g d_p}\right]^{0.327}\cdot\left(\frac{\rho_f}{\rho_s}\right)^{1.974}\cdot\left(\frac{d_p}{d_j}\right)^{-0.04}\cdot\left(-\frac{\alpha}{180}+\frac{\pi}{2}\right)^{0.148}\cdot\left(\frac{h}{h_0}\right)^{0.028} \quad (15)$$

where α stands for the nozzle inclination angle, according to the scheme in Fig. 2, while h/h_0 is the dimensionless nozzle height, i.e. the ratio of nozzle-bed surface distance to total bed height.

These cases have been analyzed as well by applying the proposed numerical procedure. Some of the results of computer simulation of lateral jet penetration into the FB, for various jet inclination angles and jet introduction heights, are shown in Figs. 5 and 6, respectively. All fluidization conditions, as well as the nozzle design, are the same as in the case of the horizontal jet analysis.

In Fig. 7 a comparison of results of numerical simulation of inclined jet penetration into the FB, and the semi-empirical experimental correlation (15) is given. As it can be observed from the diagram in Fig. 7, both the numerical simulation and the experiment point out to a weak influence of the jet inclination angle on the jet penetration length. However, the same tendency can be spotted on all diagrams – jet penetration length increases with the increase of nozzle inclination towards the bed bottom, in the observed range of values for angle α. It can be also noted from Fig. 7 that numerical simulation is in very good accordance with experimental results obtained with the inclined jet. This accordance is again more obvious for the cases with higher velocities at the nozzle exit. The same values for constants from Eq. (12) as in the case of horizontal jet ($a = 0.65$ and $b = 1.5$) were applied for this series of numerical experiments as well.

Results of the numerical calculation and experimental correlations of the influence of the nozzle-bed bottom distance on the jet penetration into the FB, for several air velocities at the nozzle outlet, are given in Fig. 8. Experimental results, as well as numerical experiments, show that the jet introduction position (h/h_0) also has a very weak influence on the jet penetration length at lower nozzle position height values, which could have been expected bearing in mind Eq. (15).

5. Modeling of the mixing of components

As it was mentioned in the Introduction, when introducing a gaseous fuel, or volatile components of a liquid fuel, into the fluidization furnace, the jet penetration length for feeding is not the only indicator of mixing of the combustion components, and therefore it is also necessary to examine the flow characteristics, diffusion and mixing intensity of gaseous components of the fuel and the oxidizer. Hence, for a more detailed analysis of the final effects of fuel jet feeding into the fluidized bed and its influence on the combustion process as a whole, in addition to observing the jet penetration length, it is desirable to monitor also the real components mixing intensity (the fuel in the nozzle and oxidizer in the fluidization gas main stream). Therefore, the proposed model of the jet penetration into the FB is supplemented by a set of transport equations for convective and diffusive mixing of gaseous components in a system that consists of the bubble phase and the dense phase (porous medium).

5.1. Chemical components mixing model

For the purpose of modeling of the chemical components mixing inside the fluidized bed, the aforementioned numerical simulation procedure (1)–(9) was expanded by incorporating an additional set of transport equations for calculating the conservation of chemical components in the system, in the following form for each gaseous component (k):

$$\frac{\partial}{\partial x_j}(\rho U_j Y_k)-\frac{\partial}{\partial x_j}\left(\varepsilon_b\rho D_k\frac{\partial Y_k}{\partial x_j}\right)=S^k, \quad (16)$$

where Y_k and D_k stand for mass fraction and diffusivity of the chemical component k, and S^k is the source/sink of the component k, having zero value in the case where there are no chemical reactions.

5.2. Simulation results for chemical components mixing in the FB

A series of numerical experiments was carried out, with mixing of the lateral jet of gaseous fuel which was introduced into the bed of particles, fluidized by the oxidizer. The working

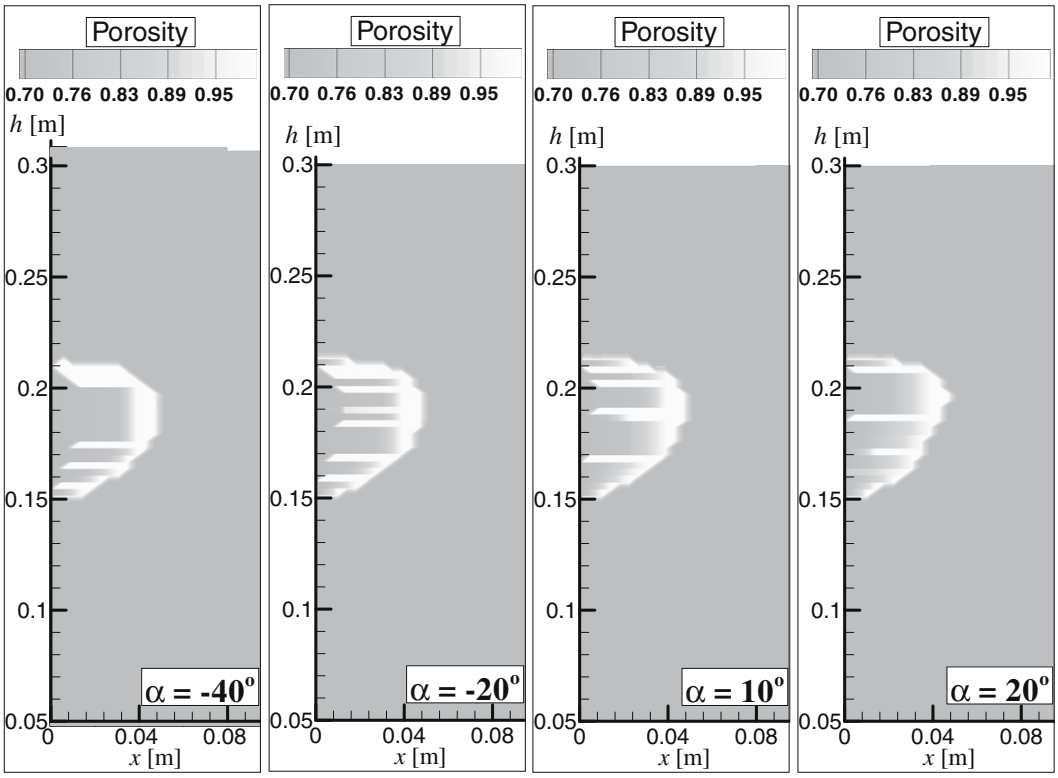

Fig. 5. Numerical simulation of lateral jet (d_j = 0.009 m, U_j = 50 m/s) penetration into the FB (ρ_s = 1402 kg/m^3, d_p = 1.43e − 3 m), for various jet inclination angles.

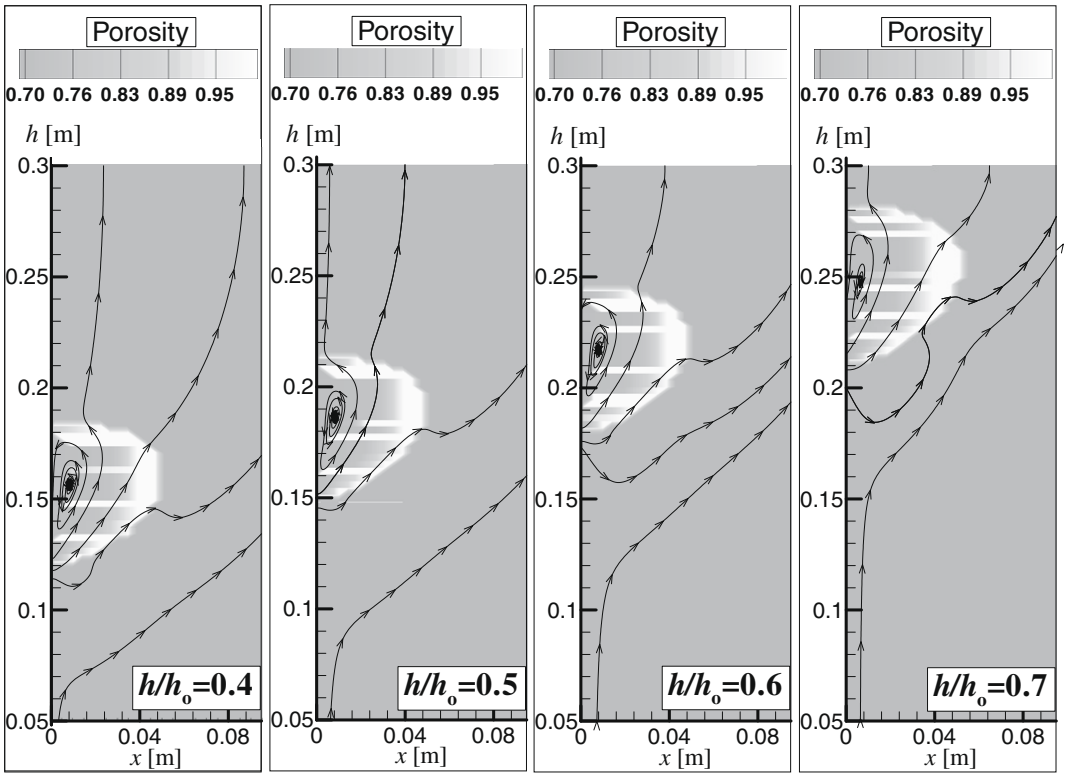

Fig. 6. Numerical simulation of lateral jet (d_j = 0.009 m, U_j = 50 m/s) penetration into the FB (ρ_s = 1402 kg/m^3, d_p = 1.43e − 3 m), for various jet introduction heights.

space geometry and FB inert material were the same as in the case of analysis of the lateral jet penetration length described in Section 3. By the procedure described in Section 5.1, mixing of two model-components, representing the fuel (entering through the nozzle) and the oxidizer, i.e. the fluidization medium, was observed.

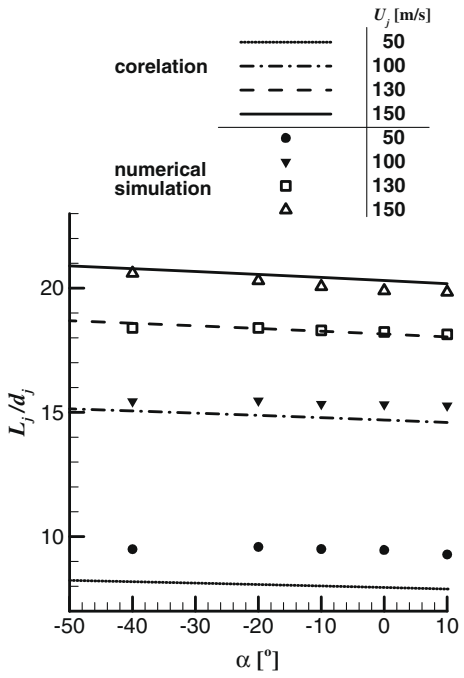

Fig. 7. Influence of the jet inclination angle on dimensionless jet penetration length.

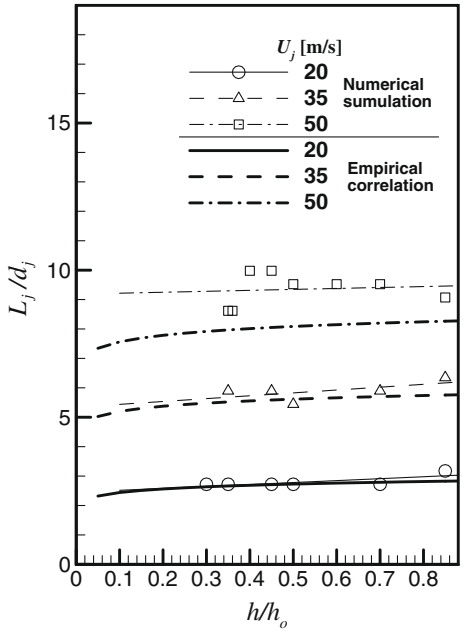

Fig. 8. Influence of the jet introduction height on dimensionless jet penetration length.

The level of mixing of the components is usually monitored by mixture fraction, which is often defined as follows:

$$f = \frac{Y_{fu} - Y_{O_2} + Y^o_{O_2}}{Y^o_{fu} + Y^o_{O_2}}, \tag{17}$$

where Y_{fu} and Y_{O_2} stand for mass fractions of the fuel and the oxidizer, in a working space point adopted at will. The index "o" denotes the mass fraction values of the components at the entry point into the working space. Considering that in the observed system there exist only two components (the fuel and the oxidizer), entering the working space separately (through the nozzle and in the form of fluidization gas, respectively), the mixture fraction is then equal to the fuel mass fraction ($f = Y_{fu}$).

Since these investigations are performed primarily with the aim to develop an efficient furnace, it is convenient to monitor the level of mixing of the components from the point of view of their stoichiometric ratio. Considering this and to improve the clarity of the results presentation, the following indicator of the desired level of mixing of the components has been adopted:

$$z = 1 - \frac{|f^{st} - f|}{f^{st}}, \tag{18}$$

where f^{st} stands for mixture fraction under the conditions of stoichiometric ratio of the components. In this way, if the value of the mixing factor defined like this (z) is closer to 1, then the components concentration ratio is closer to the ideal gas mixture.

An example of the application of the proposed numerical procedure is given in Fig. 9, in which the results of the numerical simulation of stoichiometric mixing of carbon-monoxide flow are shown. Carbon-monoxide was introduced through a horizontal nozzle (3 mm in diameter), with the velocity of 50 m/s, into the bed of particles with 1.43 mm in diameter and the material density of 1402 kg/m^3, where the material was fluidized by a stream of oxygen.

By applying the described procedure, the influences of the inlet velocity, the inclination and the position of the lateral jet of gaseous fuel on the level of stoichiometric mixing with the fluidization gas, i.e. the oxidizer, were analyzed. All fluidization conditions, as well as the nozzle design, were the same as in the case of the jet penetration length analysis (Section 4). For clearer analysis of the results of these numerical experiments, the mixing intensity of the components was quantitatively depicted through the fractions of the mixing factor stoichiometric zones (Fig. 9) in the whole working space of the furnace, i.e. of the FB. Zones with the mixing factor (z) above 0.95 were chosen as zones with "ideal mixing", i.e. zones with stoichiometric mixing level.

The Figs. 10 and 11 show the dependences of stoichiometric mixture zones fraction (i.e. the ratio of the numerically simulated working space area with $z \geqslant 0.95$, to the total working space area) on the inclination angle and the lateral jet velocity of methane and CO streams, respectively. The streams are introduced at medium height of the bed of particles fluidized by oxygen. Based on diagrams in Figs. 10 and 11 similar conclusions can be drawn as from the analysis of the experiments and of the numerical simulation of the jet penetration length into the FB, i.e. the stoichiometric mixture zones fraction strongly depends on the fuel jet entrance velocity, while the inclination angle has a small influence on the level of mixing of components. Simultaneously, the same tendency is noted as in the case of jet penetration length, i.e. the stoichiometric mixture zones fraction tends to be higher if the nozzle is more inclined towards the bed bottom.

In Fig. 12, the results of numerical simulations of the fuel and the fluidization gas mixing are shown, for the cases of several fuel-introduction heights into the fluidization furnace. Diagrams from Fig. 12 present the dependences of stoichiometric mixture zones fraction on the height and the velocity of the lateral jet of fuel (CO), which is horizontally introduced into a bed of particles fluidized by oxygen. As opposed to the analysis of the jet penetration length into the fluidization furnace, the diagrams in Fig. 12 show that the nozzle position along the FB height very strongly influences the stoichiometric mixture zones fraction. As it can be noted, a considerably higher mixing intensity of chemical components in the fluidization furnace is obtained when the lateral jet of fuel is positioned in lower zones, which could have not been concluded solely from the analysis of jet penetration length into the FB.

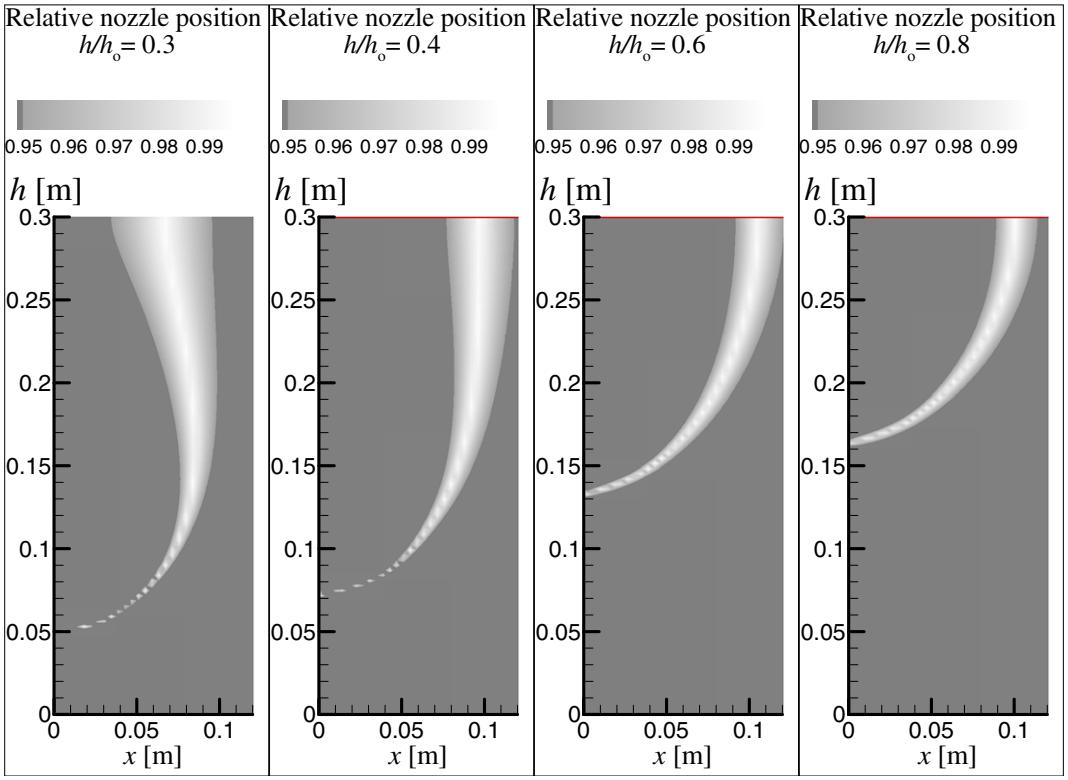

Fig. 9. Mixing factors (z) of a jet-fed fuel (CO) and the fluidization gas (O_2), for four nozzle heights inside the FB.

Nevertheless, the positioning of fuel jet feeding into the lower zones of the fluidization furnace should be done with great care in practice, because the intensity of mixing of the inert material near the FB bottom is lower which causes lower heat transfer intensity and also a non-homogeneous temperature field in this section of the bed. This may lead to the introduction of fuel into the zone with lower temperatures, which can reflect negatively to the combustion stability and efficiency, especially in the case of liquid and solid fuels.

5.3. Trial experiments with combustion of the jet-fed fuel into the FB

Trial experiments with combustion in the fluidization furnace were done on a pilot-facility, shown schematically in

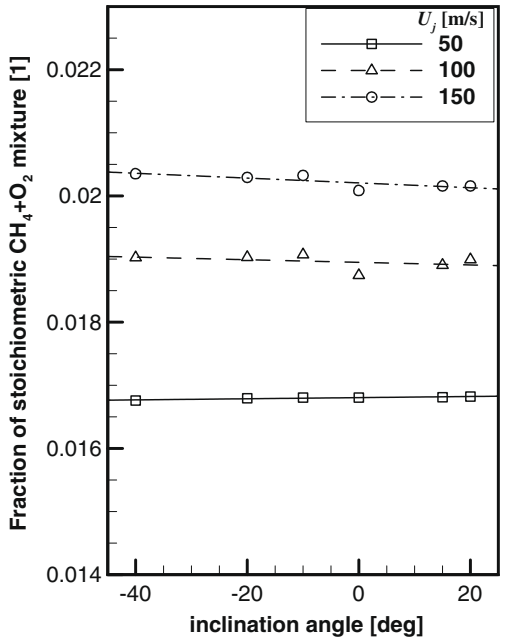

Fig. 10. Dependence of stoichiometric mixture zones fraction on the inclination angle and the lateral jet velocity of methane stream, for the nozzle diameter equal to 3 mm.

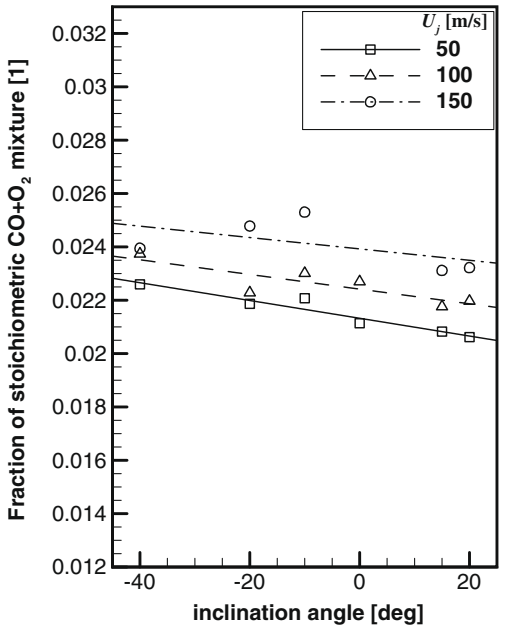

Fig. 11. Dependence of stoichiometric mixture zones fraction on the inclination angle and the lateral jet velocity of CO stream, for the nozzle diameter equal to 3 mm.

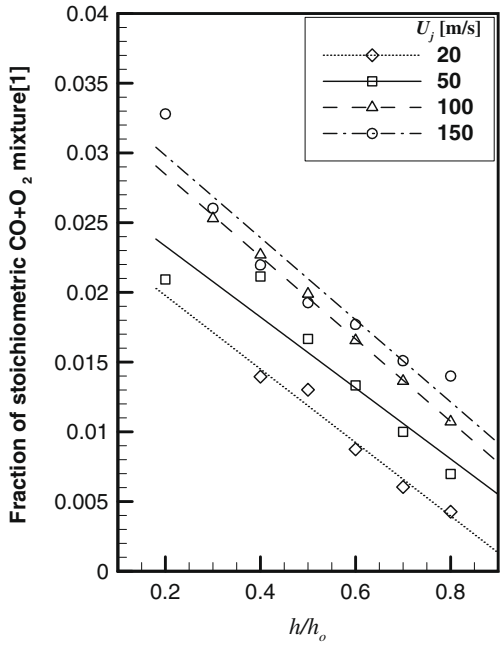

Fig. 12. Dependence of stoichiometric mixture zones fraction on the height and the lateral jet velocity of CO stream, for the nozzle diameter equal to 3 mm.

Fig. 13. The fuel (highly-volatilized oil) was fed into the FB at the angle of 38°, and it was possible to regulate the distance of the nozzle outlet from the bed bottom. The FB inert material consisted of quartz sand particles with medium diameter of 0.8 mm, deposited density of 1310 kg/m^3 and the height of 0.323 m. The fluidization gas was air. During the stationary regime of the furnace operation, temperatures inside the FB and concentrations of the combustion products were monitored continuously.

Two experiments were done at two different positions of the fuel feeding nozzle, with all other conditions of stationary combustion being the same (temperature – approximately 870 °C, air excess 2.65, the fuel mass flow rate 3.8 kg/h). The comparison of combustion efficiencies, for observed regimes of operation of the furnace with different nozzle immersing depths, was performed by monitoring CO concentrations in the flue gases. In the case when the fuel was fed at the height of 0.13 m from the bed bottom, the detected mean value of CO was 189 ppm, while in the case of feeding the fuel at the height of 0.09 m this value was only 13 ppm. The obtained data were in accordance with the conclusions drawn from the results of numerical experiments (Fig. 12), i.e. that the height at which the nozzle was positioned inside the FB strongly influenced the combustion conditions inside the fluidization furnace.

6. Conclusions

In this paper, the results of investigations carried out by applying the proposed fluid-porous medium model for fluidized bed numerical simulation are shown, where the FB dense phase is treated as a fixed porous medium. The interaction between

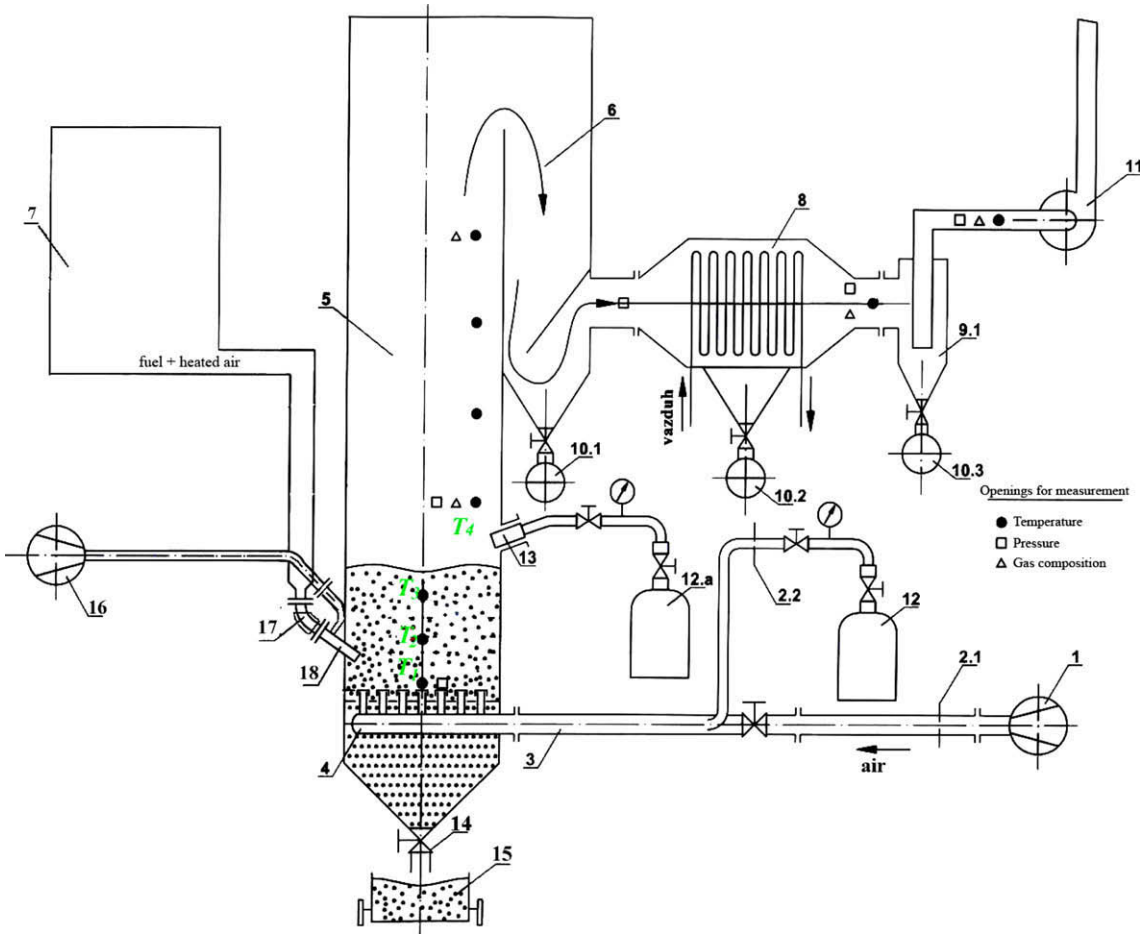

Fig. 13. Scheme of the laboratory experimental fluidization furnace with jet feeding of the fuel.

the gas and the particles, as well as the conditions for the occurrence of bubbles and non-particle zones, are modeled in a similar way as in the case of the two-fluids models, with the particle (dense phase) movement being the only aspect excluded from the simulations. The gas–particles interaction forces, similar to the two-fluids models, are reduced to the gas–particles friction force in the FB dense phase, and can be defined in accordance with the Ergun equation. The interactions between the particles themselves are reduced to the inter-particle friction force and the effects of inter-particle collisions in the FB. These two effects are modeled together, using the expression for the effective inter-particle friction force: $F_p = \psi_{fr}\rho_b(1-\varepsilon)g$. The effective friction coefficient of the particles inside the bed $\psi_{fr} = a \cdot (U_s/U_{mf})^b$, at the same time refers to the effects of the FB particle collisions. The constants a and b are the only empirical constants of the proposed model and by means of the verification based on numerous experimental results taken from literature, their values have been adopted as 0.65 and 1.5, respectively. This kind of approach to the FB modeling is suitable for rapid engineering calculations of the state of the fluidization medium, with the analysis of locations and averaged sizes of bubble phase zones, which can offer a set of useful data during the planning of processes in the FB facilities.

An example of application of the proposed FB modeling procedure is the numerical simulation of the introduction of lateral jet of fluid into the FB, i.e. prompt and simple determination of the jet penetration length into the FB, as well as the analysis of the effects of mixing of the jet-fed fuel and the fluidization medium – oxidizer. Numerical calculations have been carried out for the two-dimensional case, and the calculation results for the lateral jet penetration length were compared to numerous experimental results on two-dimensional fluidized beds, taken from literature. The lateral jet penetration length into the FB, determined by applying the proposed numerical procedure, is in very good accordance with the referent experimental values, both for horizontal jet cases and inclined jet cases, with various inclination angles. The matching of the calculations and the experiments is generally more obvious for the cases with higher velocities at the nozzle outlet.

A general conclusion of the numerical simulation and the experimental investigation is that the jet penetration length into the FB is very strongly influenced by the fluid velocity at the nozzle outlet. The jet inclination angle with respect to the horizontal position, as well as the nozzle height, have a much weaker influence on the jet penetration length into the FB. However, based on numerical experiments and on experimental investigations as well, the same tendency is observed: the jet penetration length is greater if the nozzle is more inclined towards the bed bottom, for the observed range of the jet inclination angle values (from 20° above the horizontal up to 40° below the horizontal position).

To achieve more detailed analysis of the final effects of the jet fuel feeding into the FB and its influence on the combustion process as a whole, apart from considering the jet penetration length, the real intensity of mixing of the components (fuel inside the nozzle and the oxidizer in the main stream of the fluidization gas) has been also analyzed, by applying the model of conservation of the chemical components in the FB. Based on these numerical experiments, the data obtained in the case of analyzing the influence of the nozzle outlet velocity as well as the influence of the nozzle inclination angle, are similar to the experimental results and to the results of numerical simulation of the jet penetration length into the FB, suggesting that the stoichiometric mixture zones fraction significantly depends on the inlet velocity of the fuel jet into the bed, while the inclination angle has a weak influence on the level of the components mixing. However during the analysis of the influence of the fuel introduction height, it has been shown that the nozzle position along the bed height strongly influences the mixing intensity of the chemical components in the FB, which could have not been concluded just by analyzing the jet penetration length into the FB.

The conclusions drawn from the results of numerical experiments, that the height at which the nozzle is positioned in the FB significantly influences the combustion conditions inside the fluidization furnace, are in accordance with trial experimental tests of combustion of the jet-fed fuel in the FB, done on an experimental pilot-facility with a fluidization furnace.

In the end, comparisons and certain estimations of potential agreement and discrepances can be given, with respect to more complicated models available in literature, as well as advantages and disadvantages of the numerical simulation method suggested in the paper. As already pointed out in the Introduction, Lagrangian approach to the simulation of particle motion in FB [1,2] is more exact, but it requires considerable computation time and memory capacity, so these models are more suitable for theoretical considerations of local phenomena in FB. By means of Eulerian approach, especially the two-fluid method of the FB modeling [3,4], where gas and dense phase of FB (gas–particles system at conditions of minimal fluidization velocity) are considered as two fluids with different characteristics, it is possible to provide simpler, but relatively detailed description of the transport phenomena in FB. This kind of models provides a detailed image of nonstationary distribution of the bubble phase in the FB, which, however, is not the subject of this work, so the comparison between the results of these models and the suggested one cannot be done without great difficulties.

The case treated in this paper is relatively complex. Namely, there are two gas streams, interacting with the particles: the one, aimed for the fluidization itself, and another one, the lateral jet penetrating into the FB. In addition, the gas streams have different chemical composition, while the character of their mixing is of considerable importance for the overall analysis of the process. Because of that, the model has been simplified considerably and it offers a stationary estimation of the dimensions and geometry of the jet penetrating into the FB of uniform porosity, as well as the effect of mixing of the jet and the basic fluidization stream components. On the other hand, the model does not follow the particles motion and local nonstationary occurence of the FB bubbles around the bubble zone and the jet zone. Here, it should be mentioned once again that the suggested model still takes into account one component of the particles motion, i.e. their oscillatory motion and the effects of mutual collisions within the dense phase, by means of the semi-empirical expression for effective friction coefficient (12), being a function of the fluidization number (U_s/U_{mf}) within the frame of the model (10)–(12).

In spite of a relatively simple physical model of fluidization, like it can be seen from Figs. 4, 7, and 8, 2D numerical simulation of the lateral jet penetration length into the FB, performed by means of the suggested method, agrees very well with the referent experimental data [5], for the cases of horizontal jets as well as the jets inclined at different angles.

The model of processes during the jet penetration into the FB is continuously being improved, with respect to dense phase flow modeling. An addition of chemical reactions into the model is also expected in the near future.

Acknowledgement

This work has been supported by the Ministry of Science and Technological Development (Republic of Serbia).

References

[1] J.M. Link, L.A. Cuypers, N.G. Deen, J.A.M. Kuipers, Flow regimes in a spout-fluid bed: acombined experimental and simulation study, Chem. Eng. Sci. 60 (2005) 3425–3442.
[2] R.P. Utikara, V.V. Ranade, Single jet fluidized beds: experiments and CFD simulations with glass and polypropylene particles, Chem. Eng. Sci. 62 (2007) 167–183.
[3] Alberto Di Renzo, Francesco Paolo Di Maio, Homogeneous and bubbling fluidization regimes in DEM–CFD simulations: hydrodynamic stability of gas and liquid fluidized beds, Chem. Eng. Sci. 62 (2007) 116–130.
[4] H. Enwald, E. Peiran, A.E. Almstedt, B. Leckner, Simulation of the fluid dynamics of a bubbling fluidized bed. Experimental validation of the two-fluid model and evaluation of a parallel multiblock solver, Chem. Eng. Sci. 54 (1999) 311–328.
[5] Ruoyu Hong, Hongzhong Li, Haibin Li, Yang Wang, Studies on the inclined jet penetration length in a gas–solid fluidized bed, Powder Technol. 92 (1997) 205–212.
[6] J.F. Davidson, R. Cliff, D. Harrison (Eds.), Fluidization, second ed., Academic Press, London, 1985.
[7] S.V. Patankar, Numerical Heat Transfer and Fluid Flow, Hemisphere, New York, 1980.
[8] S.V. Patankar, D.B. Spalding, A calculation procedure for heat mass and momentum transfer in three-dimensional parabolic flows, Int. J. Heat Mass Transfer 15 (1972) 1787–1806.
[9] O.M. Todes, O.B. Citovich, Apparatus with granular fluidized bed, Chemistry, St. Petersburg, 1981 (in Russian).
[10] D. Kunii, O. Levenspiel, Fluidization Engineering, Butterworth–Heinemann, London, 1991.